Journal of Applied Polymer Science

Molybdate-Doped Copolymer Coatings for Corrosion Prevention of Stainless Steel

Feng Li, Guo-xi Li, Jing Zeng, Gui-hong Gao
College of Chemistry and Chemical Engineering, Hunan University, Changsha 410082, Hunan, People's Republic of China
Correspondence to: G.-x. Li (E-mail: liguoxi@hnu.edu.cn)

ABSTRACT: The polypyrrole and polyaniline copolymer coating (PPy-PAni) and PPy-PAni doped with sodium molybdate copolymer coating (PPy-PAni-MoO_4^{2-}) were synthesized on stainless steel by cyclic voltammetry. The effect of molybdate on the passivation of stainless steel was investigated by linear sweep voltammetry in 0.2 mol L^{-1} of oxalic acid. The corrosion prevention performances of these copolymer coatings for stainless steel were investigated by linear sweep voltammetry, electrochemical impedance spectroscopy in 1 mol L^{-1} of sulfuric acid, and potentiodynamic polarization in 0.1 mol L^{-1} of hydrochloric acid. Copolymer coating doped with molybdate could accelerate the formation of the passive oxide film and have better corrosion prevention efficiencies than PPy-PAni coating on stainless steel. © 2014 Wiley Periodicals, Inc. J. Appl. Polym. Sci. **2014**, *131*, 40602.

KEYWORDS: coatings; conducting polymers; copolymers; electrochemistry

Received 21 November 2013; accepted 10 February 2014
DOI: 10.1002/app.40602

INTRODUCTION

Corrosion of metal causes enormous economy losses throughout the world, and various methods have been used for corrosion prevention. Of the several techniques, polymer coating is the most widely used and environment-protective method. Among conductive polymers (CPs), polypyrrole (PPy), and polyaniline (PAni) have been studied with interests of their electrosynthesis conditions, environmental stability, conductivity, morphology, and corrosion prevention properties.[1–5] A successful aqueous electropolymerization of CPs on steel generally requires a passive layer to prevent the dissolution of the metal before monomers are oxidized into polymers. Oxalate solution has been widely used,[6,7] because a thin layer of ferrous oxalate crystal is first formed and established the passivation of the steel substrate during the initial active dissolution; the polymer coating is formed hereafter on the steel. To enhance the corrosion prevention, a coating of CPs doped by counter anions with corrosion-inhibiting properties has been introduced. The kind of corrosion-inhibiting dopant anion such as molybdate and tungstate, which is incorporated as counter-charge ions in the polymer matrix, has a significant effect on prevention efficiencies of CPs to steel. Mascia et al.[8] reported that molybdate was doped into networks successfully in epoxy-silica hybrids and enhanced the passivation of the metal substrate for corrosion protection. Yong et al.[9] prepared a new molydbate/phosphate conversion coating on magnesium alloy, which had almost comparable corrosion protection for magnesium alloy to the traditional chromate-based coating. Karpakam et al.[10] investigated the corrosion behavior of steel with PAni-MoO_4^{2-} (PAni doped with sodium molybdate) coating in 1% of NaCl by potentiodynamic polarization and electrochemical impedance spectroscopy (EIS) techniques. It has been found that the PAni-MoO_4^{2-} coating is able to offer higher corrosion prevention in comparison with that of pure PAni coating owing to the inhibitive nature of MoO_4^{2-} ion. Sabouri et al.[11] evaluated the prevention performance of PPy-WO_4^{2-} (PPy doped with sodium tungstate) coating and PPy coating on steel in 3.5% of NaCl by EIS, revealing that PPy-WO_4^{2-} coating provided an enhancement of prevention against corrosion. The mechanism for corrosion prevention of PAni and PPy was found to be anodic passivation of the metal surface.[12–15] It would be more easy to form the passive oxide film by adding corrosion-inhibiting dopant anions and stabilizing the passive film on steel. The passive oxide film is thus formed at the steel/CP interface, decreasing the dissolution rate of steel.[10]

To provide corrosion prevention for metal, polymer coating must be a physical barrier, that is to say, the structure of the polymer must not contain large pores, and the coating can prevent anions from reaching the metal surface causing corrosion, and also prevent oxygen diffusion.[15] Most of the studies concentrated on homopolymers, and just a few investigations have been dedicated to the study of copolymers achieved by electrolyzing the solution including two monomers. Comparing electrosynthesis of homopolymers, the electrochemical deposition

of copolymer coatings is done for the improvement of the physical, chemical, mechanical, and electrical properties.[16,17] The effect of molybdate on the anticorrosion of copolymer coatings for stainless steel (SS) has not been reported.

The aim of this study is to investigate the electrochemical deposition of PPy and PAni copolymer doped with molybdate, and also importantly to study the corrosion prevention properties of PPy-PAni and PPy-PAni-MoO_4^{2-} copolymer coating for SS.

EXPERIMENTAL

Pyrrole and aniline monomers were purified by vacuum distillation and stored at low temperature in the dark prior to use. The experiments were performed by using doubly distilled water at 25 ± 1°C. The electropolymerization and corrosion test were carried out with CHI-660D electrochemical workstation and performed in three-electrode cell, saturated calomel electrode (SCE) was used as reference, and platinum foil as counter electrode. Before electrosynthesis, the 304-SS electrode (1 cm^2) was polished sequentially with 400–1200 grit emery paper, degreased with ethanol, and then washed with doubly distilled water.

The PPy-PAni copolymer on SS was electrodeposited by cyclic voltammetry in 0.075 mol L^{-1} pyrrole + 0.025 mol L^{-1} aniline + 0.2 mol L^{-1} oxalic acid. The PPy-PAni-MoO_4^{2-} copolymer was electrodeposited in the same solution but added with 0.01 mol L^{-1} of sodium molybdate. The PPy-MoO_4^{2-} and the PAni-MoO_4^{2-} homopolymers were electrodeposited in 0.1 mol L^{-1} pyrrole + 0.2 mol L^{-1} oxalic acid + 0.01 mol L^{-1} sodium molybdate and 0.1 mol L^{-1} aniline + 0.2 mol L^{-1} oxalic acid- + 0.01 mol L^{-1} sodium molybdate. The cyclic voltammetry scanning potential was cycled between −0.5 and 1.3 V versus SCE (all the electrode potentials were referred to SCE in this article) at a charge of 0.4 C cm^{-2} and at a potential sweep rate of 0.05 V s^{-1}. The coatings were slightly washed with distilled water and dried at room temperature. Infrared spectra of the copolymer coatings were recorded as KBr pellets on a Nicolet Nexus IR spectrometer. Corrosion prevention properties of these polymer-coated SS were evaluated by linear sweep voltammetry, potentiodynamic polarization, and EIS techniques. Linear sweep voltammetry was carried out at 0.02 V s^{-1} by sweeping the potential region between −0.5 and 1.5 V in 1 mol L^{-1} of sulfuric acid. The potentiodynamic polarization curves were recorded with a constant sweep rate of 0.001 V s^{-1} in 0.1 mol L^{-1} of hydrochloric acid. The EIS was performed at an amplitude of 0.008 V in the frequency range from 100 kHz to 0.01 Hz in 1 mol L^{-1} of sulfuric acid.

RESULTS AND DISCUSSION

The Effect of Molybdate on the Passivation of SS

Figure 1 shows the linear sweep voltammograms of bare SS in 0.2 mol L^{-1} of oxalic acid solution and 0.2 mol L^{-1} oxalic acid- + 0.01 mol L^{-1} sodium molybdate solution, respectively. A single forward scan from −0.5 to 1.5 V was applied with a scan rate of 0.02 V s^{-1}. The current peak at −0.22 V was the activation peak of SS. The oxalate that covered the SS surface inhibited the anodic dissolution for the low solubility of ferrous oxalate, and as a result this low solubility was followed by the precipitation of ferrous oxalate crystals. The potential of the anodic peak of SS in

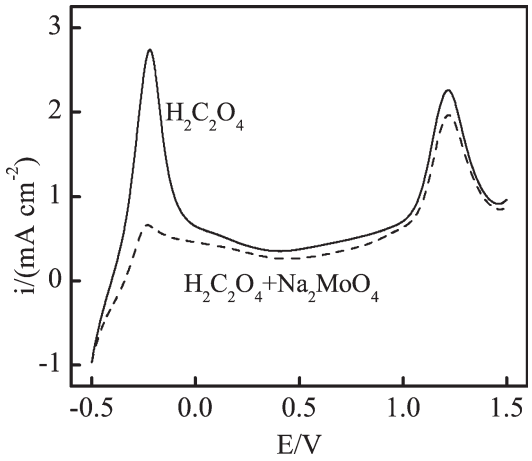

Figure 1. Linear sweep voltammetry curves of SS in 0.2 mol L^{-1} oxalic acid and 0.2 mol L^{-1} oxalic acid + 0.01 mol L^{-1} Na_2MoO_4, respectively. Scan rate: 20 mV s^{-1}.

0.2 mol L^{-1} oxalic acid + 0.01 mol L^{-1} sodium molybdate solution was the same as in 0.2 mol L^{-1} of oxalic acid. However, the anodic dissolution current was lower. The results show that molybdate can accelerate the formation of the passive oxide film, and a thin passive oxide film is more easily formed on SS, which may give a better chance to obtain the enhancement of corrosion prevention of coating doped with molybdate.

Electrosynthesis of Copolymer Coatings on SS

Figure 2 shows the cyclic voltammograms of electropolymerization of PPy-MoO_4^{2-} coating on SS in 0.1 mol L^{-1} pyrrole + 0.2 mol L^{-1} oxalic acid + 0.01 mol L^{-1} sodium molybdate, PPy-PAni copolymer in 0.075 mol L^{-1} pyrrole + 0.025 mol L^{-1} aniline + 0.2 mol L^{-1} oxalic acid, and PPy-PAni-MoO_4^{2-} copolymer in the same solution but doped with 0.01 mol L^{-1} of sodium molybdate. The oxidation potentials of two copolymers observed in the first sweep were higher than 0.9 V, which was different from pyrrole oxidation [Figure 2(a,b)] with the formation of black coating of PPy at 0.65 V. There were three prominent peaks in the cyclic voltammograms [Figure 2(c,d)]. The anodic peak at around −0.27 V was the activation peak, which was similar to the anodic dissolution of SS in 0.2 mol L^{-1} of oxalic acid or 0.2 mol L^{-1} oxalic acid + 0.01 mol L^{-1} sodium molybdate (Figure 1). However, in the second sweep, the peak disappeared, because the SS was partially coated with polymer and SS dissolution was inhibited. The anodic peak at around 0.65 V was attributed to the interconversion of PAni between leucoemeraldine and partly oxidized emeraldine state, and the anodic peaks at around 1.15 V correspond to the transition of the conducting form of emeraldine to pernigraniline state. In PPy-PAni electrosynthesis, there was a decrease of current in the 1ast cycle, indicating partial loss of electrochemical activity.

Comparing the cyclic voltammograms of PPy-MoO_4^{2-} with PPy-PAni-MoO_4^{2-}, the oxidation potential of pyrrole on SS was 0.3 V higher than pyrrole + aniline, and the current peaks at 0.65 and 1.15 V were the characteristic peaks of aniline oxidation. We arrived at a conclusion that the darkish copolymer coatings of PPy-PAni and PPy-PAni-MoO_4^{2-} were deposited successfully. The current in the case of PPy-PAni-

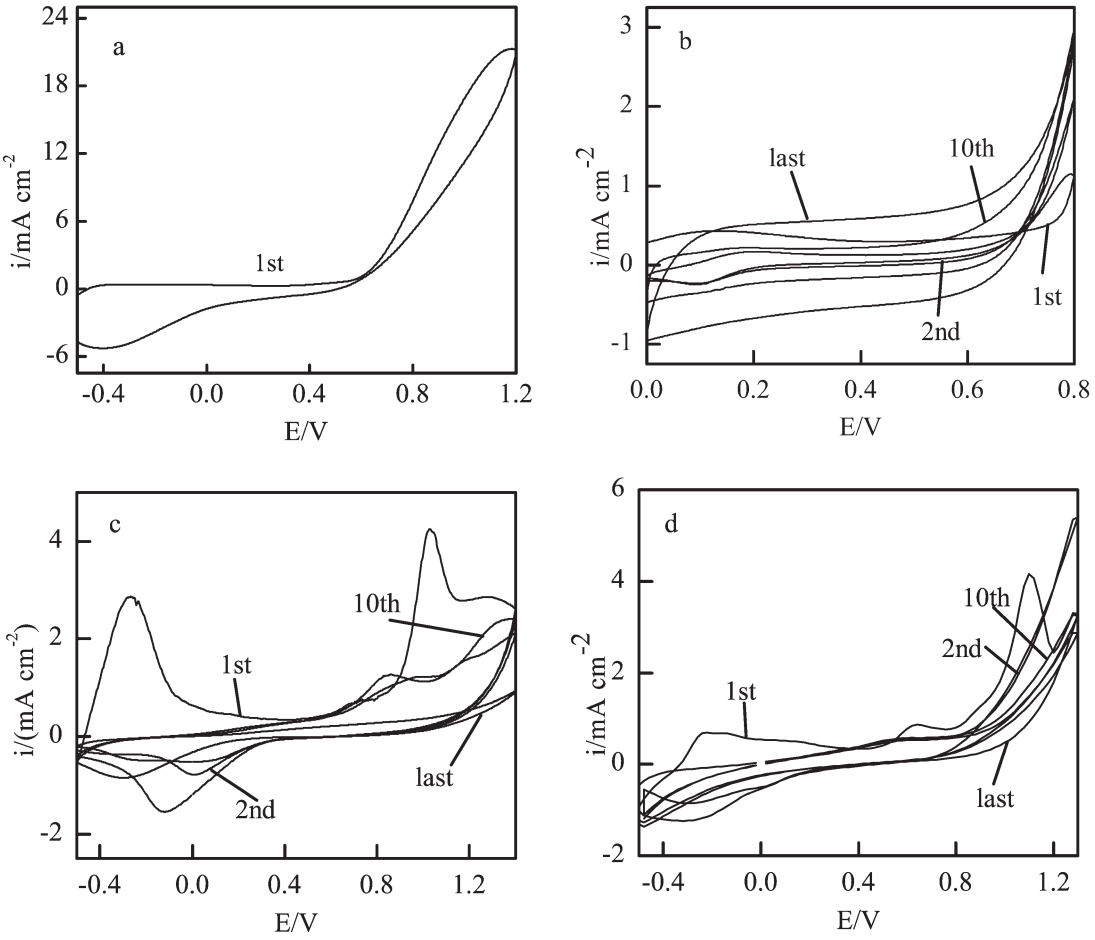

Figure 2. Cyclic voltammograms of electropolymerization of (a) PPy-MoO_4^{2-} (−0.5 to 1.2 V), (b) PPy-MoO_4^{2-} (0–0.8 V), (c) PPy-PAni, and (d) PPy-PAni-MoO_4^{2-} on SS. Polymerization charge: 0.4 C cm^{-2}, Scan rate: 50 mV s^{-1}.

MoO_4^{2-} electropolymerization was found to be higher than PPy-PAni, indicating that the initial oxidation and the growth rate of PPy-PAni-MoO_4^{2-} were more favorable than PPy-PAni. The molybdate may have a catalytic effect on the polymerization. Sun and coworkers[18] also showed that tungstate under acidic conditions acted as a catalyst for the pyrrole electropolymerization.

To investigate the effect of molybdate on the electropolymerization, PPy-PAni and PPy-PAni-MoO_4^{2-} were synthesized by chronopotentiometry at a low current density of 0.001 A cm^{-2} for 400 s (Figure 3). In the case of determining whether molybdate is present or not, different steps could be observed. In the absence of molybdate, there was an induction period for about 4 s for an active dissolution of the SS, then the potential rose, and active dissolution was inhibited gradually, as a result of the beginning of the deposition of ferrous oxalate crystals on SS. The potential began to down after 12 s attributing to the dissolution of ferrous oxalate. About 20 s later, the potential increased for the beginning of electropolymerization of monomers. It can be seen from the chronopotentiometric curve of PPy-PAni that the reaction potential was not stable in the initial part, because precipitation that occurs continuously hinders further dissolution, and at the same time the formed ferrous oxalate crystals were decomposing at this reaction time and were oxidized into highly soluble iron (III) oxalate, and also passivating iron (III) oxides deposited on the SS surface. After 130 s, the potential was stabilized and

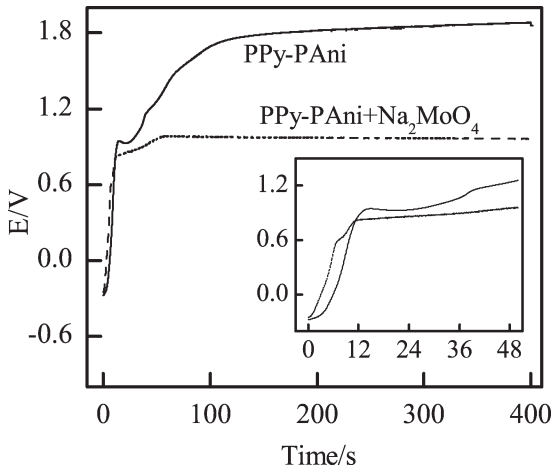

Figure 3. Chronopotentiometric curves of electrodeposition of PPy-PAni and PPy-PAni-MoO_4^{2-} on SS.

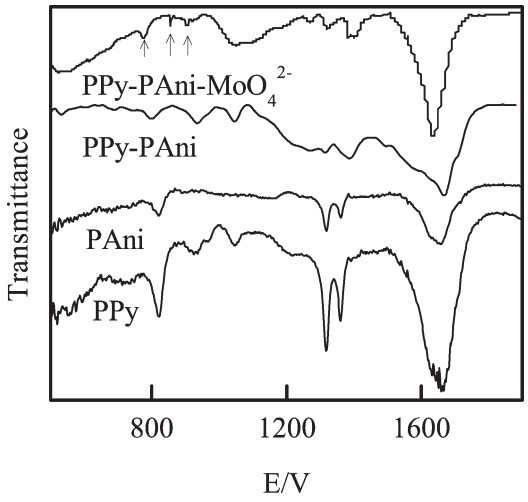

Figure 4. Infrared spectra of PPy, PAni, PPy-PAni, and PPy-PAni-MoO_4^{2-}.

copolymer coating was electrodeposited at the positive potential plateau. It can be seen that the formation process of PPy-PAni-MoO_4^{2-} occurred without an induction period in contrast to PPy-PAni, indicating that the passivation of SS was established immediately and the dissolution of SS was inhibited after applying current. Also, the electropolymerization potential of PPy-PAni-MoO_4^{2-} remains very stable and is much lower when compared with PPy-PAni, showing that the growth of PPy-PAni-MoO_4^{2-} is easier.

The Structure of Copolymers

The IR spectra of the PPy, PAni, PPy-PAni, and PPy-PAni-MoO_4^{2-} are shown in Figure 4. The bands at 773, 856, and 902 cm^{-1} correspond to stretching vibrations of the MoO_4^{2-} ion.[10,19] The sharp band at 1640 cm^{-1} is attributed to stretching vibrations of the oxidation state of the polymer or related to C═O groups of oxilic acid.[20] The bands at 1250–1500 cm^{-1} are related to stretch vibrations of C—N groups of Aromatic amine, which could be believed to be a proof of copolymerization.[21]

Evaluation of Corrosion Prevention of Copolymer Coatings

Figure 5 shows the potentiodynamic polarization curves of SS/PPy-MoO_4^{2-}, SS/PAni-MoO_4^{2-}, SS/PPy-PAni, and SS/PPy-PAni-MoO_4^{2-}, after 0-, 0.5-, 1-, and 2-h immersion in 0.1 mol L^{-1} of hydrochloric acid solution with a scan rate of 0.002 V s^{-1}. The corrosion current density (i_{corr}) calculated by the Tafel extrapolation method is listed in Table I. The i_{corr} of bare SS was 94.8 μA cm^{-2} and the E_{corr} was −0.175 V. Comparing with SS/PPy-MoO_4^{2-} and SS/PAni-MoO_4^{2-}, the i_{corr}

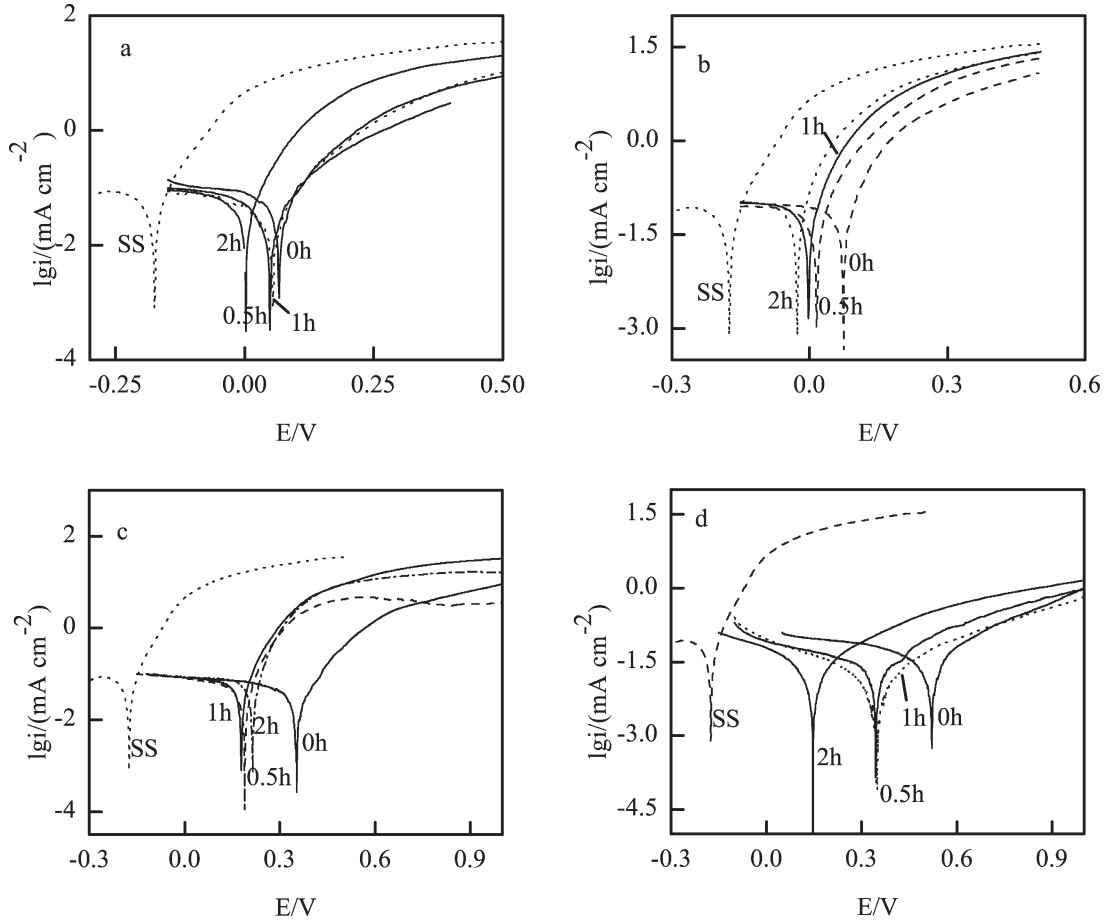

Figure 5. Potentiodynamic polarization curves of (a) SS/PPy-MoO_4^{2-}, (b) SS/PAni-MoO_4^{2-}, (c) SS/PPy-PAni, and (d) SS/PPy-PAni-MoO_4^{2-} in 0.1 mol L^{-1} of hydrochloric acid.

Table I. Potentiodynamic Polarization Parameters of SS/PPy-MoO_4^{2-}, SS/PAni-MoO_4^{2-}, SS/PPy-PAni, and SS/PPy-PAni-MoO_4^{2-} in 0.1 mol L^{-1} of Hydrochloric Acid

	Time (h)	E_{corr} (V)	i_{corr} (μA cm^{-2})
SS	0	−0.175	94.8
	0	0.066	78.8
SS/PPy-MoO_4^{2-}	0.5	0.049	77.4
	1	0.055	47.4
	2	0.002	88.0
	0	0.074	77.5
SS/PAni-MoO_4^{2-}	0.5	0.015	74.6
	1	−0.003	83.7
	2	−0.026	92.4
	0	0.350	37.7
SS/PPy-PAni	0.5	0.182	58.5
	1	0.175	82.6
	2	0.213	94.7
	0	0.518	52.6
SS/PPy-PAni-MoO_4^{2-}	0.5	0.340	39.9
	1	0.348	10.1
	2	0.146	14.6

values of SS/PPy-PAni-MoO_4^{2-} are smaller, which showed that copolymers have a better protection than homopolymers on the SS. The i_{corr} values of SS/PPy-PAni were initiated at 37.7 μA cm^{-2} and then shifted positively to the i_{corr} of bare SS of 94.7 μA cm^{-2} after 2 h, which showed that PPy-PAni completely lost the protectiveness after 2 h, whereas SS/PPy-PAni-MoO_4^{2-} exhibited a decrease of i_{corr} from 52.6 to 14.6 μA cm^{-2}. The i_{corr} values recorded for SS/PPy-PAni-MoO_4^{2-} were decreased owing to their higher barrier efficiency against the attack of corrosive media. Molybdate which is a direct passivator can strengthen, complete, and repair the passive layer.[10] In the case of the PPy-PAni-MoO_4^{2-} coating, the release of MoO_4^{2-} with self-healing properties to inhibit the corrosive attack and a significant decrease in the value of current densities were observed. Also, it is clearly seen that the corrosion potential of PPy-PAni-MoO_4^{2-}-coated SS shifted to more positive potentials with respect to SS/PPy-PAni. These results demonstrate that PPy-PAni and PPy-PAni-MoO_4^{2-} coating acts as a protective layer on steels, improves the corrosion prevention performance, and confirms the better protection when deposited copolymers were doped with MoO_4^{2-}.

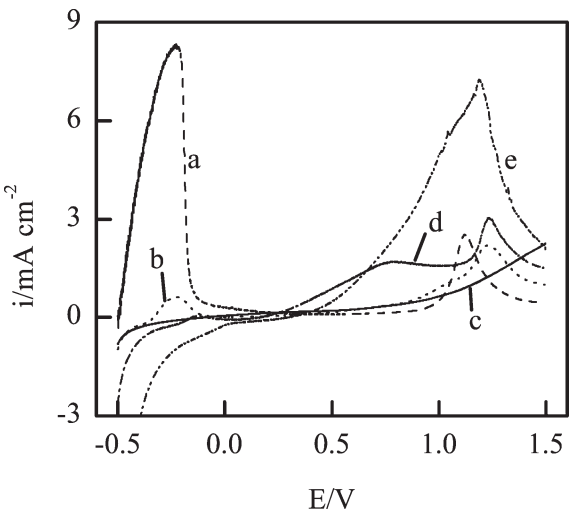

Figure 6. Linear sweep voltammetry curves of (a) SS, (b) SS/PPy-PAni, (c) SS/PPy-PAni-MoO_4^{2-}, (d) SS/PPy-MoO_4^{2-}, and (e) SS/PAni-MoO_4^{2-} in 1 mol L^{-1} of sulfuric acid. Scan range: −0.5 to 1.5 V. Scan rate: 20 mV s^{-1}.

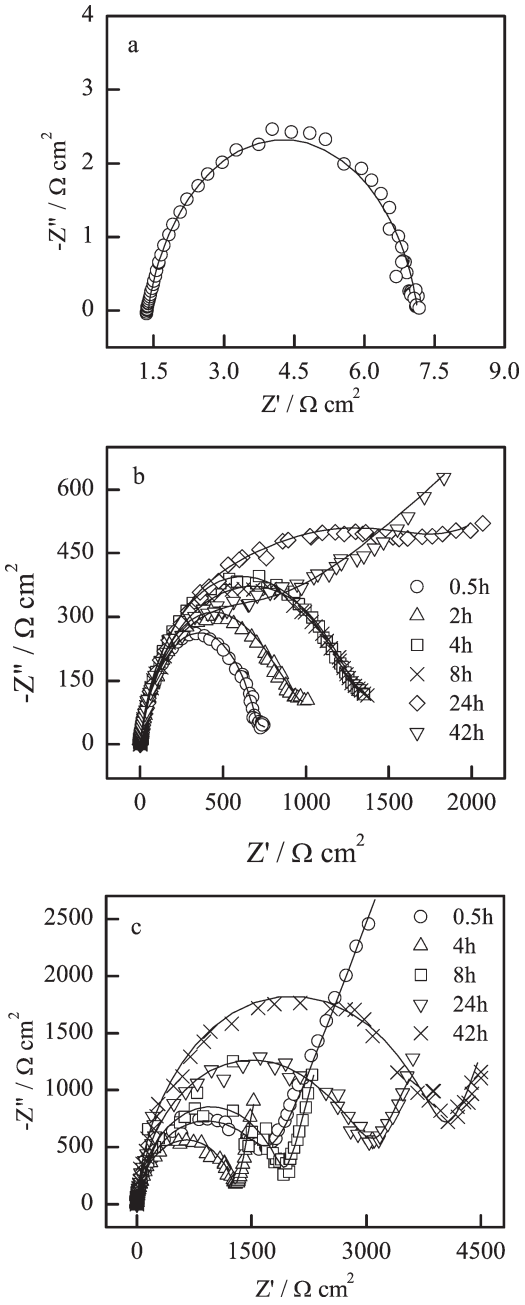

Figure 7. Nyquist plots of (a) SS, (b) SS/PPy-PAni, (c) SS/PPy-PAni-MoO_4^{2-} in 1 mol L^{-1} of sulfuric acid solution.

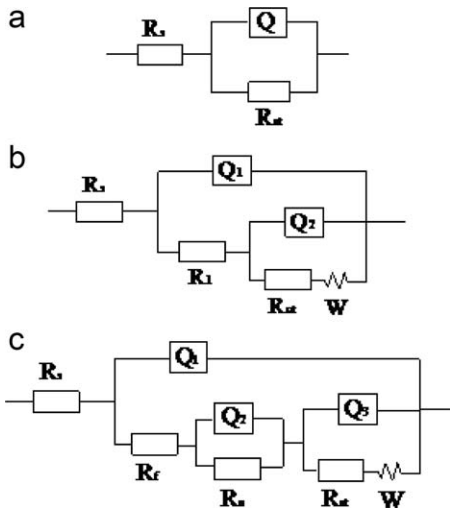

Figure 8. Equivalent circuits for the corrosion of electrodes in 0.1*M* of sulfuric acid solution. (a) uncoated SS, $Q - C_{dl}$ (double-layer capacitance); (b) SS/PPy-PAni electrodes, 0–42 h immersion, $R_1 = R_f + R_o$; SS/PPy-PAni-MoO_4^{2-}, and SS/PPy-PAni-MoO_4^{2-}/PPy-MoO_4^{2-} electrodes, <24 h of immersion. $Q_1 = C_f + C_o$, $Q_2 - C_{dl}$, $R_1 = R_f + R_o$; (c) SS/PPy-PAni-MoO_4^{2-} and SS/PPy-PAni-MoO_4^{2-}/PPy-MoO_4^{2-} electrodes, ≥24 h of immersion. Q_1–C_f, Q_2–C_o (passive layer capacitance), $Q_3 - C_{dl}$.

Figure 6 shows the linear sweep voltammetry curves of SS, SS/PPy-PAni, SS/PPy-MoO_4^{2-}, SS/PAni-MoO_4^{2-}, and SS/PPy-PAni-MoO_4^{2-} in 1 mol L^{-1} of sulfuric acid. Bare SS underwent high anodic dissolution peak at the beginning of polarization at around −0.3 V. Polymer-coated SS sharply decreased anodic current peak and underwent much less substrate dissolution. Comparing with the passive potential regions of SS/PPy-PAni and SS/PPy-PAni-MoO_4^{2-}, SS/PPy-MoO_4^{2-} and SS/PAni-MoO_4^{2-} were narrower. Especially, SS/PPy-PAni-MoO_4^{2-} showed a different behavior with SS/PPy-PAni and homopolymers owing to less dissolution that the dissolution current of SS/PPy-PAni-MoO_4^{2-} remained stable when potential is between −0.5 and 1.35 V. Consequently, the copolymers have better properties than the corresponding homopolymers and PPy-PAni-MoO_4^{2-} coatings show good protective effects for SS when compared with PPy-PAni coating in 1 mol L^{-1} of sulfuric acid solution.

The corrosion prevention performances of different coatings on SS were also investigated by EIS. Figure 7 shows the development of Nyquist plots for SS covered by PPy-PAni, PPy-PAni-MoO_4^{2-} coating in 0.1 mol L^{-1} of sulfuric acid after 0.5, 1, 2, 4, 8, 24, and 42 h of immersion, respectively. The plots had the shape of semicircle at the high frequency region and at low frequency Warburg-type impedance (W) was observed. Symbols represent experimental data, and the fitting data of impedance spectra based on equivalent circuit are given in solid lines. Equivalent circuit models are shown in Figure 8. In equivalent circuit models, R_{ct} represents the interfacial charge-transfer resistance of polymers coating, R_o is the resistance of oxide layers, R_f is the sum of the coating resistance,[22] and R_s represents the ohmic resistance of the electrolyte. A constant phase element (CPE) replaces the system capacitance (C) to describe the nonhomogeneities of the surface influenced by the morphology and composition of the electrodeposited films in system: $Z_{CPE} = [Q\ (j\omega)^n]^{-1}$, where Q is a frequency-independent constant, ω is the angular frequency, and n is the correlation coefficient ($0 < n < 1$, $n = 1$ for an ideal capacitor).[23] The fitting impedance data are summarized in Tables II and IIII.

In 0.1 mol L^{-1} of sulfuric acid, the SS resulted in anodic dissolution: $Fe \rightarrow Fe^{2+} + 2e$, and the cathodic hydrogen evolution reaction occurred in parallel: $2H^+ + 2e \rightarrow H_2$.[24] As passive film could not be formed on bare SS, the diameter of the depressed semicircles corresponds to the R_{ct}.

In comparison with bare SS, copolymer-coated SS obtained relatively high values of R_{ct}. These high R_{ct} values were related to the low charge-transfer rate between SS and conducting polymer and displayed effective protection properties.

The R_{ct} of SS/PPy-PAni in 0.1 mol L^{-1} of sulfuric acid increased with time in 24 h. This could be explained by the "auto-undoping" process as well as the formation of a passive interlayer.[25] As the polymer coating resistance and the oxide film resistance could not be resolved, the included resistance information was handled a total resistance R_1 [Figure 8(b)]. During 24 h, $C_2O_4^{2-}$ was released from coating, and the coating was reduced gradually (y is the doping degree): [PPy-PAni $(C_2O_4^{2-})_y]n + 2nye \rightarrow (PPy\text{-}PAni)n + nyC_2O_4^{2-}$, consequently, the coating conductivity decreased with time. Meanwhile, the PPy-PAni coating accelerated the oxidation of SS (ferric oxide)

Table II. Equivalent Circuit Elements of SS and SS/PPy-PAni Obtained from Fitting Data to the Equivalent Circuit Proposed in Figure 8(a,b)

	SS	SS/PPy-PAni						
	0 h	0.5 h	1 h	2 h	4 h	8 h	24 h	42 h
R_s (Ω cm^2)	1.39	1.36	1.49	1.34	1.91	1.39	1.21	1.34
Q_2 (uF cm^{-2})	724	75.9	104	19.5	88.2	86.5	83.1	66.4
n_2	0.8	0.8	1	0.72	0.61	0.65	0.84	0.86
R_{ct} (Ω cm^2)	5.8	697.2	811.7	899.2	928.7	939.2	759	303
Q_1(uF cm^{-2})		33.2	635	120	631	527	616.5	1071
N_1		0.8	1	0.73	0.62	0.65	0.59	0.23
R_1 (Ω cm^2)		2.2	81.8	198.5	314.7	493.5	1358	222.5
W (Ω cm^2)		0.045	0.041	0.016	0.003	0.004	0.006	6.16×10^{-5}

Table III. Equivalent Circuit Elements of SS/PPy-PAni+Na_2MoO_4 Obtained from Fitting Experimental Data to the Equivalent Circuit Proposed in Figure 8(b): 0.5–8 h, (c) 24–42 h

	SS/PPy-PAni+Na_2MoO_4						
	0.5h	1h	2h	4h	8h	24h	42h
R_s (Ω cm^2)	1.49	1.48	1.46	1.33	1.37	1.59	1.72
Q_3 (uF m^{-2})	44.2	46.6	49.6	50.9	50.2	34.9	5.5
n_3	0.89	0.90	0.90	0.91	0.92	0.79	1
R_{ct} (Ω cm^2)	1730	1672	1458	1293	1921	3021	3791
Q_1 (mF cm^{-2})	3.67	4.99	7.50	9.32	6.23	4.70	2.45
N_1	0.98	0.92	0.80	0.80	0.77	0.71	0.56
R_1 (Ω cm^2)	458.6	647.5	586	431.4	584.7		
R_o (Ω cm^2)						849.2	1701
W (Ω cm^2)	1.11×10^{-3}	1.10×10^{-3}	1.42×10^{-4}	1.44×10^{-4}	2.82×10^{-3}	0.066	0.11
R_f (Ω cm^2)						8.96	1
Q_2 (uF cm^{-2})						19.88	34.05
n_2						1	0.95

to stabilize the protection. The ferric oxide film also constituted a physical barrier at the bottom of pores of coating. Therefore, both the R_{ct} and the R_1 increased with time. Also, the formation of ferrous oxalate precipitates in the pores of coatings increased the impedance of the corrosion system. Up to 42 h of immersion, the value of R_{ct} decreased owing to the dissolution of ferric oxide for corrosion.

However, SS/PPy-PAni-MoO_4^{2-} exhibited a decrease of the R_{ct} value when compared with SS/PAni-PPy during 8 h, which was consistent with the phenomenon of experiments of Panaha and Danaee,[26] who gave an interpretation that the electrochemical reaction, an ion exchange between the corrosive ions and the dopants of the polymer, occurred at polymer/solution interface, whereas Hosseini et al.[27] considered that it may be owing to the diffusion of anions from coating to the interface of SS/polymer and build-up there.

After 10 h, the impedance began to increase which was similar to SS/PPy-PAni. The anodic dissolution of SS under the coating pores and the cathodic hydrogen evolution began to occur, and at the same time, the reduction of coatings as cathodic reactions was undergoing. The best fitting for the experimental data was based on a new equivalent circuit model as shown in Figure 8(c). Molybdate was incorporated into the coatings, acting as an inhibitor of the SS and also as a dopant during the electropolymerization. This protection mechanism is explained by the release of MoO_4^{2-} to stop the corrosion at defects. The MoO_4^{2-} is absorbed at the defects, by repairing those defects and leading to a more stable passivating oxide layer. MoO_4^{2-} is a very powerful corrosion inhibitor for iron, and concentrations as low as 10^{-5} mol L^{-1} cause a significant anodic shift of the corrosion potential.[26] Anion release and cation incorporation are competing parallel reactions during the reduction of coating, Paliwoda-Porebska et al.[28] observed that the cation incorporation nearly totally suppressed the anion release analyzed by X-ray photoelectron spectroscopy when PPy was doped by molybdate.

The lower value of C_{dl} reveals the higher quality of primary passive layer resulting from the participation of MoO_4^{2-} ions in primary passivation processes. The R_{ct} of the SS/PPy-PAni-MoO_4^{2-} is higher than SS/PPy-PAni, and after 42-h immersion the PPy-PAni-MoO_4^{2-} coating remains protective. PPy-PAni-MoO_4^{2-} exhibits better prevention properties than PPy-PAni.

CONCLUSIONS

Conducting copolymer coatings doped with sodium molybdate were successfully electrodeposited on SS. Molybdate has a catalytic effect on pyrrole polymerization, and active dissolution of SS was inhibited by adding molybdate into the solution.

All of the linear sweep voltammetry, the potentiodynamic polarization, and the EIS indicate coating-doped molybdate exhibited a significant protection for SS against the attack of corrosion electrolyte. Both PPy-PAni and PPy-PAni-MoO_4^{2-} coatings showed a better corrosion prevention than homopolymer coatings. Comparing with PPy-PAni coating, the prevention properties of PPy-PAni-MoO_4^{2-} coating are stronger, and the PPy-PAni coatings completely lost the protectiveness after 2-h immersion in corrosion electrolyte, whereas SS/PPy-PAni-MoO_4^{2-} exhibited an ongoing corrosion prevention.

REFERENCES

1. González, M. B.; Quinzani, O. V.; Vela, M. E.; Rubert, A. A.; Benítez, G.; Saidman, S. B. *Synth. Met.* **2012**, *162*, 1133.
2. Lehr, I. L.; Saidman, S. B. *Synth. Met.* **2009**, *159*, 1522.
3. Stejskal, J.; Bogomolova, O. E.; Blinova, N. V.; Trchová, M.; Šeděnková, I.; Prokeš, J.; Sapurina, I. *Polym. Int.* **2009**, *58*, 872.
4. Brožová, L.; Holler, P.; Kovářová, J.; Stejskal, J.; Trchová, M. *Polym. Degrad. Stab.* **2008**, *93*, 592.
5. Zhang, A.; Guo, X. *Corros. Pro.* **2003**, *24*, 428.

6. Zeybek, B.; Pekmezc, N. Ö.; Kılıç, E. *Electrochim. Acta* **2011**, *56*, 9277.
7. Mahmoudian, M. R.; Alias, Y.; Basirun, W. *J. Mater. Chem. Phys.* **2010**, *124*, 1022.
8. Mascia, L.; Prezzi, L.; Wilcox, G.; Lavorgna, M. *Prog. Org. Coat.* **2006**, *56*, 13.
9. Yong, Z.; Zhu, J.; Qiu, C.; Liu, Y. *Appl. Surf. Sci.* **2008**, *255*, 1672.
10. Karpakam, V.; Kamaraj, K.; Sathiyanarayanan, S.; Venkatachari, G.; Ramu, S. *Electrochim. Acta* **2011**, *56*, 2165.
11. Sabouri, M.; Shahrabi, T.; Faridi, H. R.; Hosseini, M. G. *Prog. Org. Coat.* **2009**, *64*, 429.
12. Zhu, R.; Li, G.; Huang, G. *Mater. Corros.* **2009**, *60*, 34.
13. Dung Nguyen, T.; Anh Nguyen, T.; Pham, M. C.; Piro, B.; Normand, B.; Takenouti, H. *J. Electroanal. Chem.* **2002**, *572*, 225.
14. Fahlman, M.; Jasty, S.; Epstein, A. J. *Synth. Met.* **1997**, *85*, 1323.
15. Herrasti, P.; Recio, F. J.; Ocón, P.; Fatás, E. *Prog. Org. Coat.* **2005**, *54*, 285.
16. Benchikh, A.; Aitout, R.; Makhloufi, L.; Saidani, B. *Desalination* **2009**, *249*, 466.
17. Iroh, J. O.; Levine, K. *J. Power Sources* **2003**, *117*, 267.
18. Hong, T.; Sun, Y. H.; Jepson, W. P. *Corros. Sci.* **2002**, *44*, 101.
19. Lehr, I. L.; Saidman, S. B. *Electrochim. Acta* **2006**, *51*, 3249.
20. Hasanor, R.; Bilgic, S. *Prog. Org. Coat.* **2009**, *64*, 435.
21. Bekir, S.; Muzaffer, T. *Synth. Met.* **1998**, *94*, 221.
22. Ozyılmaz, A. T.; Erbil, M.; Yazıcı, B. *Thin Solid Films* **2006**, *496*, 431.
23. Castagno, K. R. L.; Azambuja, D. S.; Dalmoro, V. *J. Appl. Electrochem.* **2009**, *39*, 93.
24. Grgur, B. N.; Živković, P.; Gvozdenović, M. M. *Prog. Org. Coat.* **2006**, *56*, 240.
25. Tallman, D. E.; Pae, Y.; Bierwagen, G. P. *Corrosion* **2000**, *56*, 401.
26. Panaha, N. B.; Danaee, I. *Prog. Org. Coat.* **2010**, *68*, 214.
27. Hosseini, M. G.; Sabouri, M.; Shahrabi, T. *Prog. Org. Coat.* **2007**, *60*, 178.
28. Paliwoda-Porebska, G.; Rohwerder, M.; Stratmann, M.; Rammelt, U.; Duc, L. M.; Plieth, W. *J. Solid State Electrochem.* **2006**, *10*, 730.